AD-A082 386 AIR FORCE GEOPHYSICS LAB HANSCOM AFB MA F/G 4/1

LINEAR FILTERING ON THE SURFACE OF A SPHERE.(U)

OCT 79 R SHAPIRO

UNCLASSIFIED AFGL-TR-79-0263 NL

END

DATE FILMED

4 80

DTIC

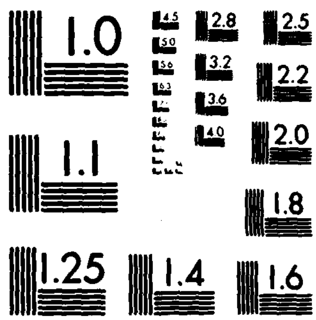

MICROCOPY RESOLUTION TEST CHART
NATIONAL BUREAU OF STANDARDS-1963-A

Unclassified

SECURITY CLASSIFICATION OF THIS PAGE (When Data Entered)

REPORT DOCUMENTATION PAGE

READ INSTRUCTIONS BEFORE COMPLETING FORM

1. REPORT NUMBER AFGL-TR-79-0263 (14) AFGL-ERP-683 · 2. GOVT ACCESSION NO.	3. RECIPIENT'S CATALOG NUMBER
4. TITLE (and Subtitle) (6) LINEAR FILTERING ON THE SURFACE OF A SPHERE.	5. TYPE OF REPORT & PERIOD COVERED Scientific. Interim.
	6. PERFORMING ORG. REPORT NUMBER ERP No. 683
7. AUTHOR(s) (10) Ralph Shapiro	8. CONTRACT OR GRANT NUMBER(s)
9. PERFORMING ORGANIZATION NAME AND ADDRESS Air Force Geophysics Laboratory (LY) Hanscom AFB Massachusetts 01731	10. PROGRAM ELEMENT, PROJECT, TASK AREA & WORK UNIT NUMBERS (16) 61102F 2310 (17) G2
11. CONTROLLING OFFICE NAME AND ADDRESS Air Force Geophysics Laboratory (LYD) Hanscom AFB Massachusetts 01731	12. REPORT DATE (11) 29 October 1979
	13. NUMBER OF PAGES 33
14. MONITORING AGENCY NAME & ADDRESS (if different from Controlling Office) (12) 34	15. SECURITY CLASS. (of this report) Unclassified
	15a. DECLASSIFICATION/DOWNGRADING SCHEDULE

16. DISTRIBUTION STATEMENT (of this Report)

Approved for public release; distribution unlimited.

17. DISTRIBUTION STATEMENT (of the abstract entered in Block 20, if different from Report)

(9) Environmental research papers,

18. SUPPLEMENTARY NOTES

DTIC ELECTE MAR 28 1980 S D B

19. KEY WORDS (Continue on reverse side if necessary and identify by block number)

Numerical weather prediction
High order filter
Spherical geometry
Scale dependent filter

20. ABSTRACT (Continue on reverse side if necessary and identify by block number)

Although methods of filtering have been developed for representing on a planar surface the sub-grid scale process of diffusion in numerical modeling of the atmosphere, the proper form of filtering for a spherical domain remains to be selected. In this study, the characteristics of several different forms of a highly scale dependent low pass filter are examined and compared for the case where the filter is applied to a scalar field on the surface of a sphere. The phase and amplitude response functions of the various forms of the filter → next page

DD FORM 1 JAN 73 1473 EDITION OF 1 NOV 65 IS OBSOLETE

Unclassified

SECURITY CLASSIFICATION OF THIS PAGE (When Data Entered)

409578

20. Abstract (Continued)

indicate that the simplest form, although it does not preserve area-weighted mean values, approaches most closely the criteria established for the ideal filter. This indication is verified by test computations in which each form of the filter is applied up to 10,000 times to a noisy scalar field.

Preface

I wish to express my thanks to Donald Aiken for his skillful handling of the computations and to Helen Connell for her efficiency in converting manuscript to typescript.

Contents

Illustrations

Linear Filtering on the Surface of a Sphere

1. INTRODUCTION

An efficient and useful filter has been developed to represent the sub-grid scale process of diffusion in numerical models of the atmosphere (Shapiro[1]). The filter has the property of variable-scale dependency. That is, as the order of the operator is increased, the dissipation of the short wavelength components is increased relative to that of the longer wavelengths. The operator of order 8 effectively eliminates components with wavelengths less than 4-grid intervals but produces no measurable damping of components with wavelengths greater than 6-grid intervals (Shapiro[2]). When used in numerical models of the atmosphere, the filter promotes computational stability by removing the highly noise contaminated short waves (particularly the 2-grid-interval wave) but because of its scale dependency does not damp the longer, meteorologically important wave components (Hunt,[3] Francis,[4] Voice and Hunt,[5] Tapp and White,[6] Mudrick,[7, 8] Kalnay-Rivas et al[9]). Consequently, use of the filter minimizes the unfortunate tendency of all stable models to suppress the growth of baroclinic instability and eddy-kinetic energy.

(Received for publication 29 October 1979)

Due to the number of references to be included as footnotes on this page, the reader is referred to the list of references, page 33.

There is no ambiguity in the use of the filter in a grid system which is mapped on a tangent plane or on polar stereographic coordinates. The proper form of the filter is developed from the linear finite difference analogue of the second derivative in space or time. However it is not at all clear what the proper form of the filter is in spherical geometry, because of both the convergence of the meridians and the potential mathematical singularity at the poles. The purpose of this study is to examine a variety of possible filter forms in order to derive a rational basis for selection of a best form.

The one-dimensional operator of order p = 1, 2, 3, ... given by

$$f_i^{(p)} = \left[1 + (-1)^{p+1} \left(\frac{\delta}{2}\right)^{2p}\right] f_i \qquad (1)$$

where $\delta^2 f_i$ is represented as a finite difference analogue of the second derivative of f (in space or time) at the gridpoint i multiplied by the square of the space or time increment. The above operator has been shown to be a useful scale-dependent filter (Shapiro[2]). For any integer $p \geq 1$ the filter removes 2 grid-interval components completely and becomes increasingly scale dependent as p increases. With a suitable choice of the form of δ^2, the filter preserves the phase of all Fourier components, introduces no new components nor does it amplify any existing component. It is therefore highly effective as a dissipative and diffusive mechanism (Shapiro[1]). It is particularly useful in any highly repetitive or iterated procedure such as the numerical marching procedures of numerical weather prediction (NWP) models. Although there is no confusion concerning the appropriate form of δ^2 in one dimension with uniform gridspacing or in more than one dimension in Cartesian coordinates, there are a variety of forms that δ^2 may assume when applied on the surface of a sphere.

Francis[4] has applied the filter in a form in which δ^2 is an analogue of the finite difference representation of the second derivative in the north-south direction on a sphere. This form has the property of conserving area-weighted mean quantities and with a suitable choice of grid location and spacing it is self-consistently well-behaved at the poles. Kalnay-Rivas, et al[9] have compared the above form of the filter with the Cartesian form which neglects the spherical geometry and a simpler, but not consistent version of the spherical form. They found little difference among the three forms although only the form suggested by Francis[4] is consistent with the spherical geometry.

Since the properties of the filter are largely determined by the form of δ^2 this paper explores the characteristics of the filter with various forms of δ^2 as applied to operations on the surface of a sphere.

2. FORMS OF δ^2

If the function $g(x, y, z)$ in rectangular Cartesian coordinates is expressed in spherical coordinates in terms of $f(\theta, \lambda, r)$ we have

$$\begin{aligned} x &= r \cos\theta \cos\lambda \\ y &= r \cos\theta \sin\lambda \\ z &= r \sin\theta \end{aligned} \tag{2}$$

where r is the distance from the origin normal to the surface of the sphere, θ is the latitude measured positive northward from the equator and λ is the longitude, measured positive toward the east. The LaPlacian of g or f is given by

$$\nabla^2 g = \left(\frac{\partial^2}{\partial x^2} + \frac{\partial^2}{\partial y^2} + \frac{\partial^2}{\partial z^2} \right) g = \nabla^2 f \ ,$$

where

$$\nabla^2 f = (r^2 \cos^2 \theta)^{-1} \frac{\partial^2 f}{\partial \lambda^2} + (r^2 \cos\theta)^{-1} \frac{\partial}{\partial \theta} \left(\cos\theta \frac{\partial f}{\partial \theta} \right) + r^{-2} \frac{\partial}{\partial r} \left(r^2 \frac{\partial f}{\partial r} \right) \tag{3}$$

Let f_{ij} represent the function f on the surface of a sphere at the gridpoint (ij) where i is an index for λ and j an index for θ. $\Delta\lambda$ and $\Delta\theta$, the grid increments in the i and j directions, are constants in space though not necessarily equal to each other. The first and second terms on the right of (3) represent respectively the variation of f in the east-west direction along a latitude circle and in the north-south direction along a meridian. If we restrict attention to the surface of a sphere, the third term is zero. In applying the filter (1) to the field of f_{ij} in the east-west direction, there is no ambiguity concerning the choice of δ^2. We have

$${}_i\delta^2 f_{ij} = f_{i+1,j} - 2f_{ij} + f_{i-1,j} \tag{4}$$

where the subscript to the left of δ^2 indicates the direction of the filtering. We have examined the following forms of ${}_j\delta^2 f_{ij}$

Form 1

$$f_{i,j+1} - 2f_{ij} + f_{i,j-1}$$

Form 2

$$\frac{1}{\cos\theta_j}\left[(f_{i,j+1} - f_{ij})\cos\theta_{j+1/2} - (f_{ij} - f_{i,j-1})\cos\theta_{j-1/2}\right]$$

Form 3

$$\frac{1}{\cos\theta_j}\left[f_{i,j+1}\cos\theta_{j+1} - 2f_{ij}\cos\theta_j + f_{i,j-1}\cos\theta_{j-1}\right]$$

Form 4

$$f_{i,j+1} - 2f_{ij} + f_{i,j-1} - \frac{\Delta\theta}{2}(f_{i,j+1} - f_{i,j-1})\tan\theta_j$$

Form 5

$$f_{i,j+1} - 2f_{ij} + f_{i,j-1} + (f_{i,j+1} - f_{i,j-1})(\cos\theta_{j+1} - \cos\theta_{j-1})/4\cos\theta_j$$

Form 1 is the Cartesian form and avoids singularities at the poles by neglecting the spherical geometry. Forms 2, 4 and 5 are finite difference versions of the second term on the right of (3). Form 3 is an arbitrary simplification of Form 2. Forms 2 to 5 all have potential singularities at the poles, but if the gridpoints j are chosen so that the north and south poles are situated at 1/2-grid interval north and south respectively of the most northerly or southerly gridpoint j, then Form 2 used by Francis,[4] has no singularity and may be applied in a self-consistent fashion. Some arbitrariness is unavoidable near the poles with the use of the other forms.

3. PHASE AND AMPLITUDE RESPONSE

The order p amplitude response of the filter (1) with the use of Form 1 for δ^2 has been shown (Shapiro[1]) to be

$$R_1 = 1 - \sin^{2p}\alpha \tag{5}$$

where $\alpha = n\Delta/2$, n is the wave number of the Fourier component whose wavelength is given by $\lambda = 2\pi/n$ and Δ is the gridspacing. Equation (5) shows that no Fourier component can be amplified by the filter, that the wave of length 2Δ is removed regardless of the value of p and that as p increases the highest wave number for which there is virtually no damping also increases. Therefore the filter becomes increasingly scale dependent as p increases. That is, the maximum slope of the amplitude response function becomes increasingly steep, thus effectively distinguishing between those frequencies which suffer virtually no damping from those which are almost completely damped. The phase response or phase shift of this form of the filter is zero since this form is symmetrical. This important property ensures that no new Fourier components are introduced merely by filtering. These desirable properties of the filter do not obtain with any of the other forms of δ^2. The phase (ϕ) and amplitude response (R) functions for the filter (1) with Forms 2 to 5 of δ^2 and with p = 1 are given below

Form 2:

$$\phi_2 = \tan^{-1}\left[\frac{\sin\alpha\cos\alpha\sin\left(\frac{\Delta\theta}{2}\right)\tan\theta_j}{1-\sin^2\alpha\cos\left(\frac{\Delta\theta}{2}\right)}\right] \tag{6}$$

$$R_2 = \left\{\left[1-\sin^2\alpha\cos\left(\frac{\Delta\theta}{2}\right)\right]^2 + \sin^2\alpha\cos^2\alpha\sin^2\left(\frac{\Delta\theta}{2}\right)\tan^2\theta_j\right\}^{1/2} \tag{7}$$

Form 3:

$$\phi_3 = \tan^{-1}\left[\frac{\sin 2\alpha\sin\Delta\theta\tan\theta_j}{1+\cos 2\alpha\cos\Delta\theta}\right] \tag{8}$$

$$R_3 = \frac{1}{2}\left\{[1+\cos 2\alpha\cos\Delta\theta]^2 + \sin^2 2\alpha\sin^2\Delta\theta\tan^2\theta_j\right\}^{1/2} \tag{9}$$

Form 4:

$$\phi_4 = \tan^{-1}\left(\frac{\Delta\theta}{2}\tan\alpha\tan\theta_j\right) \tag{10}$$

$$R_4 = \left[\cos^4\alpha + \sin^2\alpha\cos^2\alpha\tan^2\theta_j\left(\frac{\Delta\theta}{2}\right)^2\right]^{1/2} \tag{11}$$

Form 5:

$$\phi_5 = \tan^{-1}\left(\frac{1}{2}\sin\Delta\theta\tan\alpha\tan\theta_j\right) \tag{12}$$

$$R_5 = \left(\cos^4\alpha + \frac{1}{4}\sin^2\alpha\cos^2\alpha\tan^2\theta_j\sin^2\Delta\theta\right)^{1/2} \tag{13}$$

Although in the limit as α approaches zero (and in the case of Form 3 as $\Delta\theta$ also approaches zero) the forms of the filter (Forms 2 to 5) have the same amplitude response and phase shift as Form 1, in each case for non-zero values of α and $\Delta\theta$ the phase shift is different from zero everywhere except at $\theta_j = 0$. Furthermore, the phase shift is a function of latitude and wave number. This means that application of the filter (Forms 2 to 5) to a function with a single Fourier component will introduce new Fourier components merely by the filtering process. In addition the amplitude response is not only a function of wave number, as it should be, but also a function of latitude. Beyond this, and potentially more serious is the fact that the amplitude response of the filter (with Forms 2 to 5) is a function of $\tan^2\theta_j$ which becomes increasingly large as θ_j approaches $\pm\pi/2$. This feature of Forms 2 to 5 introduces the possibility that the filter could actually amplify certain Fourier components.

If we assume that θ_j is chosen so that it does not include the poles ($\theta = \pm\pi/2$), then the maximum value of $\tan^2\theta_j$ (and therefore tne maximum value of R for Forms 2 to 5) occurs when $\theta_j = \pm 1/2\,(\pi - \Delta\theta)$. That is, for these Forms R is a maximum for θ_j 1/2-grid interval from the poles. But $\tan^2[\pm 1/2\,(\pi - \Delta\theta)] = \text{ctn}^2(\Delta\theta/2)$. Therefore, the maximum value of (7)

$$R_2\,(\max) = \left\{1 - \sin^2\alpha\cos\left(\frac{\Delta\theta}{2}\right)\left[2 - \cos\left(\frac{\Delta\theta}{2}\right)\right]\right\}^{1/2} \tag{14}$$

Since $0 \leq \cos(\Delta\theta/2)\,[2 - \cos(\Delta\theta/2)] \leq 1$, $R_2^2(\max) \leq 1$ and approaches R_1^2 as $(\Delta\theta/2) \to 0$. Nevertheless, R_2 is a function of θ_j and this property as well as the phase shift that occurs with the Form 2 filter will introduce false, extraneous Fourier components. The fact that R_2 is well-behaved in terms of not amplifying any existing component implies that the extraneous components will remain small. This feature does not obtain with R_3 (max) which is given by

$$R_3\,(\max) = \left\{\left[\sin^2\alpha + \cos^2\left(\frac{\Delta\theta}{2}\right)\right]^2 - 4\sin^4\alpha\cos^2\left(\frac{\Delta\theta}{2}\right)\right\}^{1/2} \tag{15}$$

For reasonable values of $\Delta\theta$, (for example, $\Delta\theta < 11^{\circ}$), $\cos^2(\Delta\theta/2) > 0.99$. With $\cos^2(\Delta\theta/2) = 0.99$, R_3 (max) > 1 for $0.0102 < \sin^2\alpha < 0.6587$, which includes the bulk of the Fourier components of interest.

R_4 (max) is given by

$$R_4\,(\max) = \left\{(1 - \sin^2\alpha)\left(1 - \sin^2\alpha\left[1 - \frac{\left(\frac{\Delta\theta}{2}\right)^2\cos^2\left(\frac{\Delta\theta}{2}\right)}{\sin^2\left(\frac{\Delta\theta}{2}\right)}\right]\right)\right\}^{1/2} \tag{16}$$

Inasmuch as the quantity $0 \leq (\Delta\theta/2)^2 \cos^2(\Delta\theta/2)/\sin^2(\Delta\theta/2) \leq 1$, it is apparent that R_4^2 (max) ≤ 1. Similarly, the closely related R_5 (max) which is given by

$$R_5\,(\max) = \left\{(1 - \sin^2\alpha)\left(1 - \sin^2\alpha\left[1 - \cos^4\left(\frac{\Delta\theta}{2}\right)\right]\right)\right\}^{1/2} \tag{17}$$

can easily be seen to satisfy the condition R_5^2 (max) ≤ 1.

It appears that although all forms of the filter with the possible exception of Form 3 can be expected to behave reasonably well, only Form 1 exhibits no potentially pathological behavior. It is of interest therefore to compare the various forms of the filter in severe, but realistic circumstances.

4. TEST COMPARISONS

For purposes of test comparison we make use of a convenient scalar function of latitude (θ) and longitude (λ) which had been used by Yee[10] in another study. This function has the form

$$f(\lambda, \theta) = \sin\theta\left\{A + \sum_{m=1}^{18} B(m)\cos^m\theta\cos m\lambda\,[1 + \alpha(m) + \beta(\theta)]\right\} \tag{18}$$

where A is a constant, B is a weighting factor which is a function of m, the wave number parameter, and α and β are random phase shifts. $f(\lambda, \theta)$ was evaluated with a resolution of $\Delta\theta = \Delta\lambda = 2\pi/36$, yielding values for f_{ij} for i = 1, 2, ..., 36 corresponding to λ = 0, 10, ..., 350 deg and j = 1, 2, ..., 18, 19, ..., 36 corresponding to θ = -85, -75, ..., 85, 85, ..., -85 deg. Thus gridpoints (i, j), for which

10. Yee, S.Y.K. (1978) An Efficient Barotropic Vorticity Equation Model on a Sphere, Env. Res. Pap. No. 645, AFGL-TR-78-0273, AD A065 117.

$1 \le j \le 18$, are on the ith meridian, but gridpoints for which $19 \le j \le 36$ are on the $(i + 18)$th meridian. Together, these gridpoints form a complete meridian circle. f_{ij} is therefore doubly periodic with $i = i \pm 36$ and $j = j \pm 36$. Since there are only 648 (18 times 36) distinct values of f_{ij} each distinct value is assigned twice. That is $f_{ij} = f_{i+18, 37-j}$. f_{ij} was treated in this fashion so as to permit the calculation of the double Fourier spectrum. The field f_{ij} $(j = 1, 2, \ldots, 18)$ is shown in Figure 1. f_{ij} has been scaled so that $-1 < f_{ij} < 1$, although for our purposes the numerical value of f_{ij} is less important than its spatial or spectral distribution. It can be seen from Figure 1 that f is "noisy" with abrupt variations between relative maxima and minima. This "noisy" appearance is consistent with its two-dimensional Fourier spectrum shown in Figure 2 which indicates that an appreciable fraction of the total variance of f_{ij} is contained in wave numbers 9 to 18 corresponding to wavelengths from 4- to 2-grid intervals.

We also make use of a modified function, $f^*(\lambda, \theta)$, given by

$$f^*(\lambda, \theta) = f(\lambda, \theta) \cos \theta \tag{19}$$

which is illustrated in Figure 3 and whose two-dimensional Fourier spectrum is shown in Figure 4. The principal difference between f^*_{ij} and f_{ij} is the much smaller variation of f^*_{ij} with respect to longitude near polar latitudes. In this regard f^*_{ij} is more consistent with the spherical geometry. Because of the relatively large amount of variance at high wave numbers, both f_{ij} and f^*_{ij} represent severe tests of the effectiveness of the filter.

In applying the filter to f_{ij} and f^*_{ij} we use the form of δ^2 given by (4) in the i-direction regardless of the form used in the j-direction. In general, the one-dimensional operator of order p, Eq. (1), can be applied as a sequence of p, 3-point operations or as a single $(2p + 1)$ - point operation. Because of the special treatment required near the poles it was convenient to apply the operation in both the i and j directions as sequences of 3-point operations. In order to evaluate ${}_j\delta^2 f_{ij}$, it is necessary to have available values at $f_{i, j+1}$ and $f_{i, j-1}$ as well as at f_{ij}. When $j = 1$ or 18, $f_{i, j-1}$ and $f_{i, j+1}$ respectively are considered to be the gridpoints across the poles situated at $f_{i+18, j}$. This expedient, which is not necessary in the case of Form 2, was adopted primarily because it seems reasonable to treat the poles, insofar as possible, in the same fashion as any other point. However, some tests were carried out in which the poles were treated as quasi-solid boundaries with generally unsatisfactory results.

Two-dimensional filtering may consist of different orders of filtering in each direction, consistent with the two-dimensional Fourier spectrum of the field being operated upon. However, for the present study the same order of filtering (with $p = 8$) was used for all f_{ij} for both the i and j directions. Filtering was first

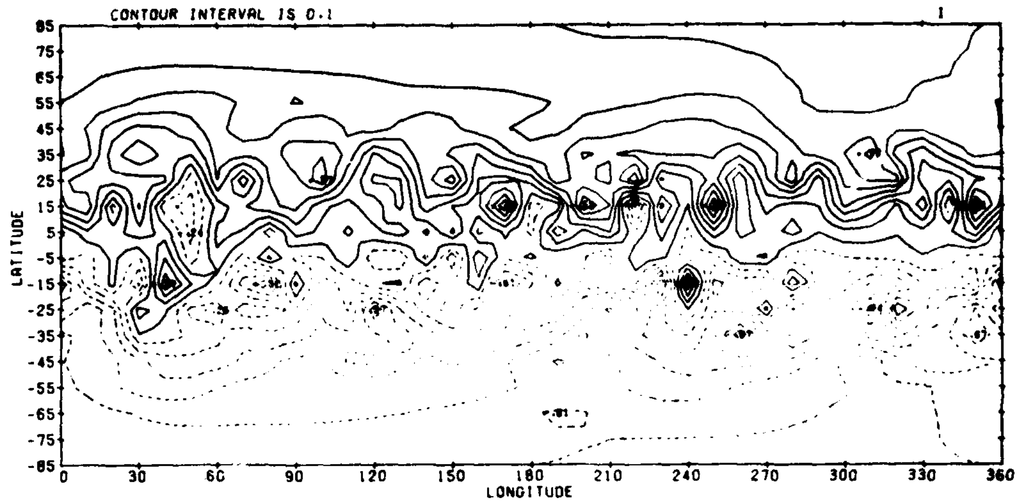

Figure 1. Initial, Unsmoothed Stream Function Field, f_{ij}

100 X INITIAL 2-DIMENSIONAL FOURIER WAVE NUMBER SPECTRUM

WAVE NUMBER E-W

WAVE NUMBER N-S	0	1	2	3	4	5	6	7	8	9	10	11	12	13	14	15	16	17	18
0	0	0	19	0	2	0	17	0	19	0	17	0	16	0	29	0	10	0	4
1	1080	7	62	17	36	17	21	26	8	29	10	0	5	11	9	30	7	9	5
2	0	94	5	69	5	42	22	35	15	16	17	3	14	23	32	10	12	17	5
3	0	3	62	4	49	4	35	18	18	9	24	9	7	4	22	25	20	7	16
4	0	5	20	36	9	39	16	39	17	14	15	3	3	35	15	17	8	26	4
5	0	6	4	22	10	19	18	5	16	12	27	13	8	5	26	21	27	10	26
6	0	3	12	12	2	21	8	13	32	6	24	10	15	32	10	20	2	24	5
7	0	4	2	21	8	26	16	19	15	16	21	5	22	12	22	17	30	11	34
8	0	3	2	4	10	12	25	14	21	17	15	21	16	18	15	19	4	14	3
9	0	5	3	5	15	10	17	25	14	19	12	4	25	12	14	7	26	12	37
10	0	4	5	2	6	3	16	19	16	10	11	25	12	10	17	10	9	3	3
11	0	3	8	20	27	20	16	13	10	33	3	1	15	9	5	11	14	18	31
12	0	4	7	8	7	14	14	16	34	4	23	15	6	18	13	1	11	12	14
13	0	1	2	14	11	23	9	9	10	37	6	11	8	12	3	21	3	22	17
14	0	5	2	15	4	18	30	16	24	8	27	13	1	20	8	8	11	19	19
15	0	1	11	2	25	14	9	16	17	29	13	14	29	15	8	21	19	18	0
16	0	0	5	2	15	15	20	11	5	5	20	43	3	17	4	11	6	23	14
17	0	3	11	3	42	14	24	10	20	11	17	6	44	7	10	9	28	7	11
18	0	4	0	10	0	10	0	5	0	2	0	40	0	10	0	9	0	17	0

Figure 2. Two-Dimensional Fourier Spectrum of Initial Field, f_{ij}, Multiplied by 100

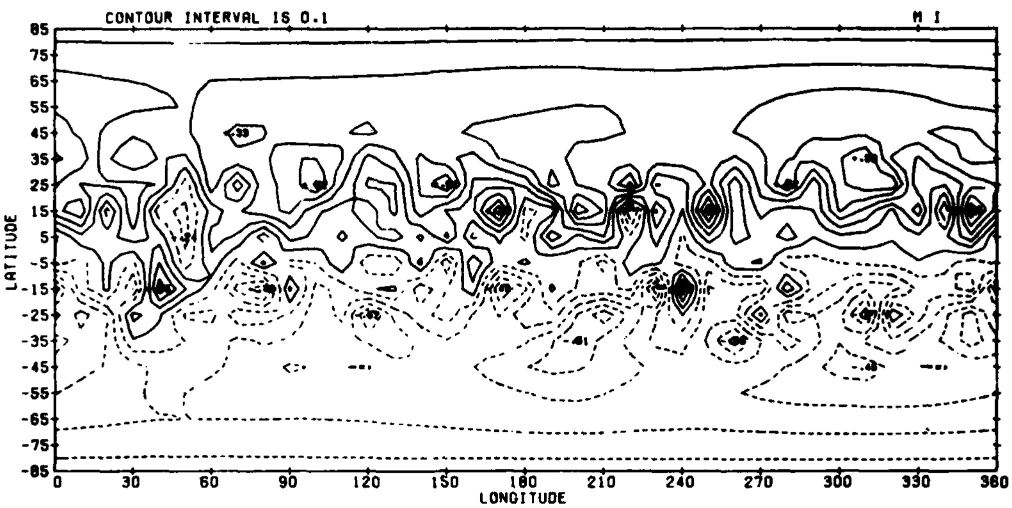

Figure 3. Unsmoothed, Modified Stream Function Field, f^*_{ij}

100 X INITIAL 2-DIMENSIONAL FOURIER WAVE NUMBER SPECTRUM

WAVE NUMBER N-S \ WAVE NUMBER E-W	0	1	2	3	4	5	6	7	8	9	10	11	12	13	14	15	16	17	18
0	0	0	14	0	2	0	17	0	17	0	15	0	14	0	27	0	10	0	4
1	460	6	42	14	27	14	17	25	7	26	9	1	4	10	8	29	7	8	5
2	0	64	5	54	5	36	21	31	14	13	15	2	13	21	31	10	12	16	5
3	273	2	55	3	42	3	30	17	16	9	22	8	5	4	21	24	19	7	16
4	0	18	15	37	7	37	13	35	16	12	14	3	2	33	14	16	8	24	5
5	64	5	12	19	13	18	19	4	16	10	26	11	8	5	25	20	26	10	26
6	0	5	12	12	1	21	8	13	29	5	21	11	13	31	8	19	2	23	5
7	29	3	0	17	5	23	16	17	15	14	21	5	21	11	22	16	29	10	33
8	0	3	2	3	8	11	22	11	18	14	14	20	15	18	14	18	4	13	3
9	16	3	2	4	15	8	16	22	14	19	12	3	23	11	14	7	24	12	36
10	0	3	4	1	5	3	13	16	15	9	10	23	12	10	16	10	9	4	4
11	9	3	5	17	23	16	15	14	9	31	4	1	14	8	5	10	13	17	30
12	0	2	5	8	5	12	13	15	30	3	22	13	6	17	13	0	11	11	13
13	6	0	2	13	8	18	7	10	10	35	6	10	9	11	3	20	3	20	17
14	0	3	1	12	4	16	27	15	23	7	25	14	1	19	8	7	10	18	18
15	3	2	6	2	23	11	9	14	17	28	12	13	28	13	7	20	18	17	1
16	0	0	3	2	11	15	19	11	7	5	18	41	2	17	4	11	6	22	13
17	1	1	8	2	40	10	22	8	20	11	17	6	42	6	10	8	27	6	10
18	0	3	0	7	0	10	0	6	0	2	0	37	0	11	0	8	0	17	0

Figure 4. Two-Dimensional Fourier Spectrum of Modified Field, f^*_{ij}, Multiplied by 100

completed in the i-direction and then these partly filtered values were filtered in the j-direct using one of the 5 Forms listed in Section 2.

For simplicity the two-dimensional filtering operation making use of Eq. (4) for $i\delta^2$ and Form ( ) for $j\delta^2$ will be referred to as a Form ( ) filter.

Figures 5 to 7 and 8 to 10 show the result of applying the Form 1, 2 and 3 filters (to f_{ij}) 1000 and 10,000 times respectively. Examination of Figures 5 to 7 shows a remarkable change brought about by the filtering as compared with the initial field (Figure 1). The filtered fields are smooth. Furthermore, the differences among the three forms are small, except for Form 3 at high latitudes. The misbehavior of Form 3 at high latitudes was anticipated by Eq. (15). Comparison of Figures 5 to 7 with Figures 8 to 10 shows that after 1000 applications of any of the three forms little further filtering takes place.

Figures 11 to 16 show the two-dimensional Fourier spectra of the filtered results shown in Figures 5 to 10 respectively. Figures 11 to 16 confirm the conclusions derived from Figures 5 to 10, but in addition they clearly reveal other characteristics of various forms of the filter.

For our purposes, an ideal filter would remove high wave number components both in the i- and j-directions, would preserve the phase and amplitude of lower wave number components and would not create any components which were not present before filtering. Although all three forms of the filter are highly effective in removing the high wave number components in the i (east-west) direction, only Form 1 is equally effective in the j-direction. Furthermore only Form 1 succeeds in avoiding the amplification of existing components or introducing new components, although Form 2 is obviously superior to Form 3.

Figures 17 to 22 show the result of filtering the f^*_{ij} field (Figure 3) with the Form 1, 2, and 3 filters. These figures are comparable to Figures 5 to 10 respectively except for the cos θ modification of the initial field. The comments made concerning Figures 5 to 10 apply with equal force to Figures 17 to 22. Judging from these figures, there would appear to be little basis for choosing among the 3 forms of the filter except for the simplicity of Form 1. However, Figures 23 to 25 and Figures 26 to 28 which show the two-dimensional Fourier spectra of the f^*_{ij} fields expressed as percentages of the original spectrum after 1000 and 10,000 applications of the Form 1, 2 and 3 filters demonstrate the superiority of the Form 1 filter. This form of the filter appears to have the characteristics of the ideal filter outlined above.

Figures 29 to 32 show the comparable two-dimensional Fourier spectra of the f^*_{ij} fields after filtering with Forms 4 and 5 respectively. Forms 4 and 5 appear to have characteristics which are similar to those of Form 2. This is not surprising in view of the similarity of their phase and amplitude response functions.

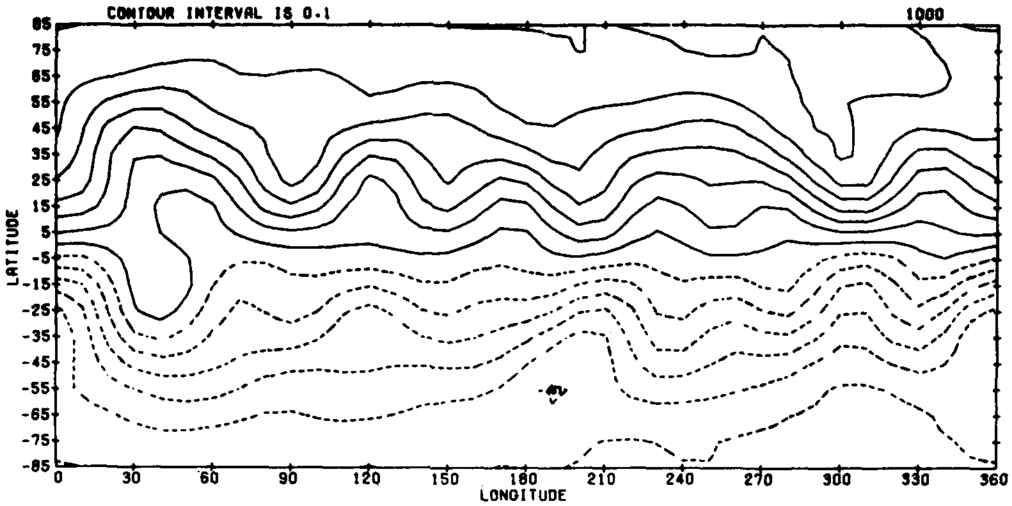

Figure 5. f_{ij} **After 1000 Applications of the Form 1 Filter**

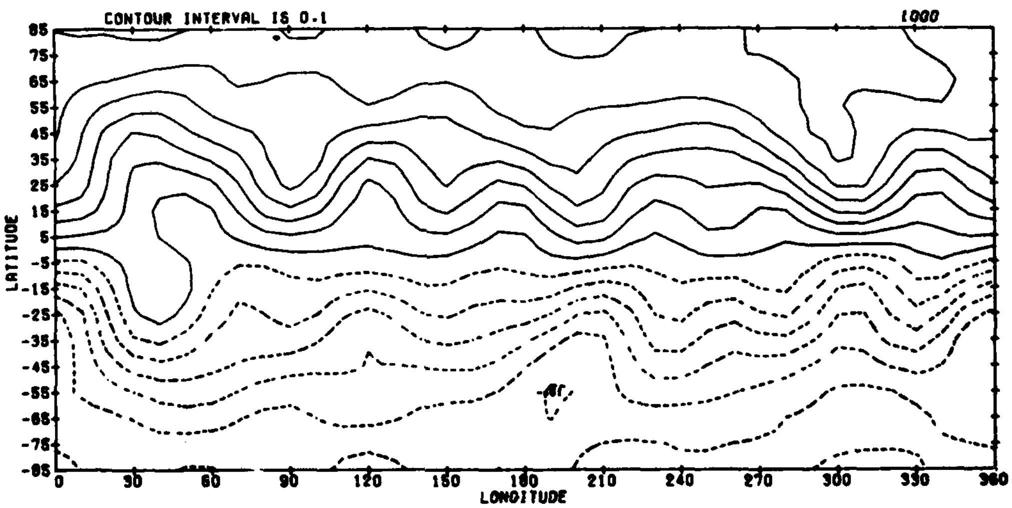

Figure 6. f_{ij} **After 1000 Applications of the Form 2 Filter**

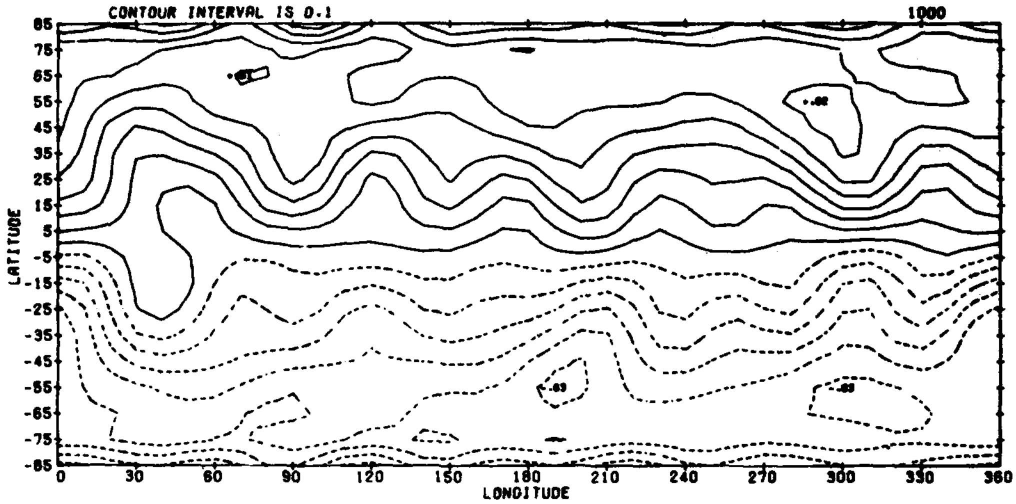

Figure 7. f_{ij} **After 1000 Applications of the Form 3 Filter**

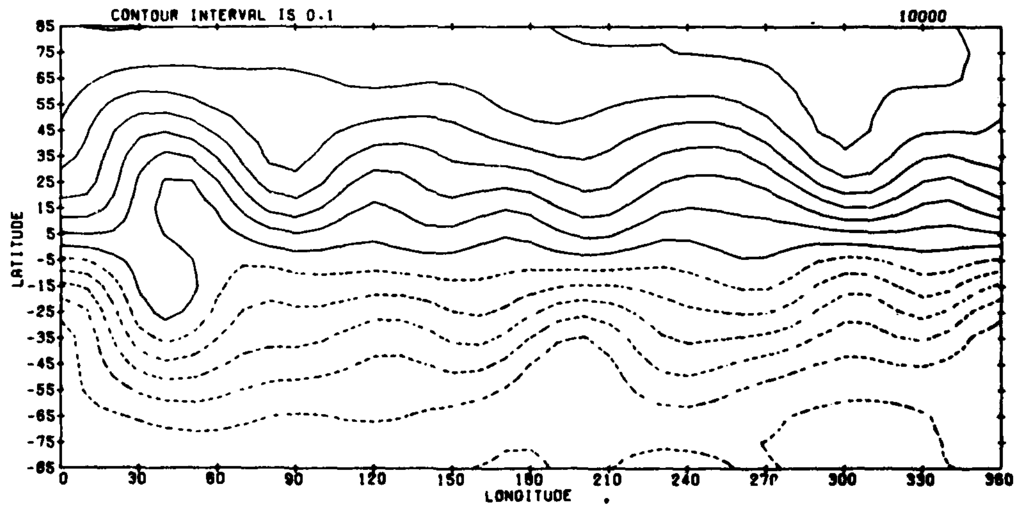

Figure 8. f_{ij} **After 10,000 Applications of the Form 1 Filter**

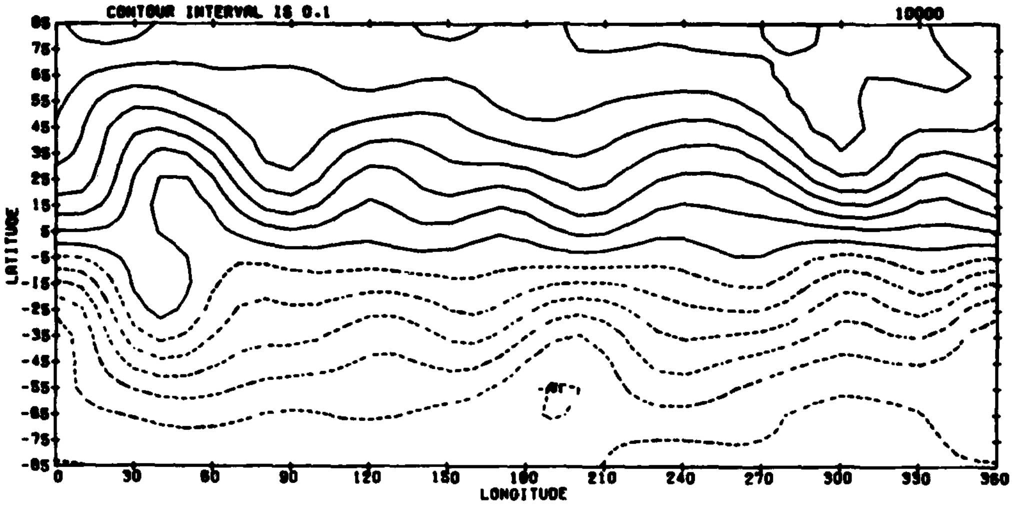

Figure 9. f_{ij} **After 10,000 Applications of the Form 2 Filter**

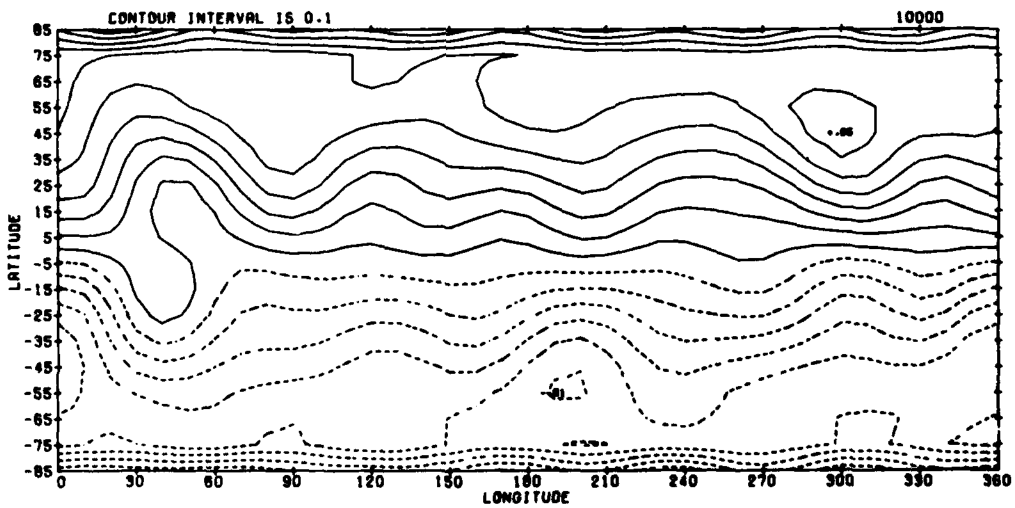

Figure 10. f_{ij} **After 10,000 Applications of the Form 3 Filter**

100 X 2-DIMENSIONAL FOURIER ANALYSIS 1000 SMOOTHINGS FORM 1

WAVE NUMBER E-W

WAVE NUMBER N-S	0	1	2	3	4	5	6	7	8	9	10	11	12	13	14	15	16	17	18
0	0	0	19	0	2	0	17	0	8	0	0	0	0	0	0	0	0	0	0
1	1080	7	62	17	36	17	21	23	4	1	0	0	0	0	0	0	0	0	0
2	0	94	5	69	5	42	22	30	7	0	0	0	0	0	0	0	0	0	0
3	0	3	62	4	49	4	34	16	8	0	0	0	0	0	0	0	0	0	0
4	0	5	20	36	9	39	16	34	7	0	0	0	0	0	0	0	0	0	0
5	0	6	4	22	10	19	18	4	7	0	0	0	0	0	0	0	0	0	0
6	0	3	12	12	2	21	8	11	14	0	0	0	0	0	0	0	0	0	0
7	0	3	1	18	7	22	14	14	6	0	0	0	0	0	0	0	0	0	0
8	0	1	1	2	4	5	11	5	4	0	0	0	0	0	0	0	0	0	0
9	0	0	0	0	0	0	0	0	0	0	0	0	0	0	0	0	0	0	0
10	0	0	0	0	0	0	0	0	0	0	0	0	0	0	0	0	0	0	0
11	0	0	0	0	0	0	0	0	0	0	0	0	0	0	0	0	0	0	0
12	0	0	0	0	0	0	0	0	0	0	0	0	0	0	0	0	0	0	0
13	0	0	0	0	0	0	0	0	0	0	0	0	0	0	0	0	0	0	0
14	0	0	0	0	0	0	0	0	0	0	0	0	0	0	0	0	0	0	0
15	0	0	0	0	0	0	0	0	0	0	0	0	0	0	0	0	0	0	0
16	0	0	0	0	0	0	0	0	0	0	0	0	0	0	0	0	0	0	0
17	0	0	0	0	0	0	0	0	0	0	0	0	0	0	0	0	0	0	0
18	0	0	0	0	0	0	0	0	0	0	0	0	0	0	0	0	0	0	0

Figure 11. Two-Dimensional Fourier Spectrum (× 100) of f_{ij} After 1000 Applications of the Form 1 Filter

100 X 2-DIMENSIONAL FOURIER ANALYSIS 1000 SMOOTHINGS FORM 2

WAVE NUMBER E-W

WAVE NUMBER N-S	0	1	2	3	4	5	6	7	8	9	10	11	12	13	14	15	16	17	18
0	0	0	19	0	2	0	19	0	10	0	0	0	0	0	0	0	0	0	0
1	1080	7	62	17	36	17	19	23	3	1	0	0	0	0	0	0	0	0	0
2	0	94	5	69	4	42	17	30	5	0	0	0	0	0	0	0	0	0	0
3	0	3	62	4	50	4	36	16	8	0	0	0	0	0	0	0	0	0	0
4	0	5	20	36	12	39	21	34	5	0	0	0	0	0	0	0	0	0	0
5	0	6	5	22	11	19	16	4	6	0	0	0	0	0	0	0	0	0	0
6	0	3	13	12	3	21	15	12	17	0	0	0	0	0	0	0	0	0	0
7	0	3	2	19	7	24	16	16	6	0	0	0	0	0	0	0	0	0	0
8	0	2	0	4	2	7	5	9	1	0	0	0	0	0	0	0	0	0	0
9	0	2	0	7	0	7	0	3	0	0	0	0	0	0	0	0	0	0	0
10	0	2	0	2	0	2	0	5	0	0	0	0	0	0	0	0	0	0	0
11	0	1	0	5	0	5	0	3	0	0	0	0	0	0	0	0	0	0	0
12	0	2	0	2	0	1	0	4	0	0	0	0	0	0	0	0	0	0	0
13	0	1	0	4	0	5	0	3	0	0	0	0	0	0	0	0	0	0	0
14	0	2	0	2	0	1	0	3	0	0	0	0	0	0	0	0	0	0	0
15	0	1	0	3	0	4	0	3	0	0	0	0	0	0	0	0	0	0	0
16	0	2	0	2	0	1	0	3	0	0	0	0	0	0	0	0	0	0	0
17	0	1	0	3	0	4	0	2	0	0	0	0	0	0	0	0	0	0	0
18	0	2	0	1	0	1	0	2	0	0	0	0	0	0	0	0	0	0	0

Figure 12. Two-Dimensional Fourier Spectrum (× 100) of f_{ij} After 1000 Applications of the Form 2 Filter

100 X 2-DIMENSIONAL FOURIER ANALYSIS 1000 SMOOTHINGS FORM 3

WAVE NUMBER E-W

WAVE NUMBER N-S	0	1	2	3	4	5	6	7	8	9	10	11	12	13	14	15	16	17	18
0	0	0	20	0	3	0	19	0	11	0	0	0	0	0	0	0	0	0	0
1	1115	7	61	17	38	18	18	24	4	1	0	0	0	0	0	0	0	0	0
2	0	95	3	69	4	43	19	31	5	0	0	0	0	0	0	0	0	0	0
3	37	3	64	4	47	5	39	11	9	0	0	0	0	0	0	0	0	0	0
4	0	5	18	36	10	38	18	33	3	0	0	0	0	0	0	0	0	0	0
5	41	7	6	21	15	14	11	10	5	0	0	0	0	0	0	0	0	0	0
6	0	5	15	13	3	25	13	14	20	0	0	0	0	0	0	0	0	0	0
7	52	2	5	21	13	33	25	29	10	0	0	0	0	0	0	0	0	0	0
8	0	3	4	5	6	3	11	12	4	0	0	0	0	0	0	0	0	0	0
9	69	0	4	8	6	15	11	14	4	0	0	0	0	0	0	0	0	0	0
10	0	4	3	4	2	3	3	6	3	0	0	0	0	0	0	0	0	0	0
11	58	0	2	6	4	11	7	11	3	0	0	0	0	0	0	0	0	0	0
12	0	4	2	3	1	3	2	5	2	0	0	0	0	0	0	0	0	0	0
13	43	0	2	5	3	9	5	9	2	0	0	0	0	0	0	0	0	0	0
14	0	4	1	2	1	2	1	4	2	0	0	0	0	0	0	0	0	0	0
15	26	0	1	4	1	8	3	9	1	0	0	0	0	0	0	0	0	0	0
16	0	4	0	2	0	2	0	4	1	0	0	0	0	0	0	0	0	0	0
17	9	0	0	4	0	8	1	8	0	0	0	0	0	0	0	0	0	0	0
18	0	2	0	2	0	2	0	3	0	0	0	0	0	0	0	0	0	0	0

Figure 13. Two-Dimensional Fourier Spectrum (× 100) of f_{ij} After 1000 Applications of the Form 3 Filter

100 X 2-DIMENSIONAL FOURIER ANALYSIS 10000 SMOOTHINGS FORM 1

WAVE NUMBER E-W

WAVE NUMBER N-S	0	1	2	3	4	5	6	7	8	9	10	11	12	13	14	15	16	17	18
0	0	0	19	0	2	0	15	0	0	0	0	0	0	0	0	0	0	0	0
1	1080	7	62	17	36	17	18	7	0	0	0	0	0	0	0	0	0	0	0
2	0	94	5	69	5	42	19	9	0	0	0	0	0	0	0	0	0	0	0
3	0	3	62	4	49	4	30	5	0	0	0	0	0	0	0	0	0	0	0
4	0	5	20	36	9	39	14	10	0	0	0	0	0	0	0	0	0	0	0
5	0	6	4	21	10	19	15	1	0	0	0	0	0	0	0	0	0	0	0
6	0	3	11	10	2	18	6	3	0	0	0	0	8	0	0	0	0	0	0
7	0	1	0	5	2	6	4	1	0	0	0	0	0	0	0	0	0	0	0
8	0	0	0	0	0	0	0	0	0	0	0	0	0	0	0	0	0	0	0
9	0	0	0	0	0	0	0	0	0	0	0	0	0	0	0	0	0	0	0
10	0	0	0	0	0	0	0	0	0	0	0	0	0	0	0	0	0	0	0
11	0	0	0	0	0	0	0	0	0	0	0	0	0	0	0	0	0	0	0
12	0	0	0	0	0	0	0	0	0	0	0	0	0	0	0	0	0	0	0
13	0	0	0	0	0	0	0	0	0	0	0	0	0	0	0	0	0	0	0
14	0	0	0	0	0	0	0	0	0	0	0	0	0	0	0	0	0	0	0
15	0	0	0	0	0	0	0	0	0	0	0	0	0	0	0	0	0	0	0
16	0	0	0	0	0	0	0	0	0	0	0	0	0	0	0	0	0	0	0
17	0	0	0	0	0	0	0	0	0	0	0	0	0	0	0	0	0	0	0
18	0	0	0	0	0	0	0	0	0	0	0	0	0	0	0	0	0	0	0

Figure 14. Two-Dimensional Fourier Spectrum (× 100) of f_{ij} After 10,000 Smoothings of the Form 1 Filter

100 X 2-DIMENSIONAL FOURIER ANALYSIS 10000 SMOOTHINGS FORM 2

WAVE NUMBER E-W

WAVE NUMBER N-S	0	1	2	3	4	5	6	7	8	9	10	11	12	13	14	15	16	17	18
0	0	0	18	0	2	0	16	0	0	0	0	0	0	0	0	0	0	0	0
1	1080	7	62	17	33	17	19	7	0	0	0	0	0	0	0	0	0	0	0
2	0	94	6	69	4	42	16	9	0	0	0	0	0	0	0	0	0	0	0
3	0	3	62	4	52	4	29	5	0	0	0	0	0	0	0	0	0	0	0
4	0	5	22	36	12	39	18	10	0	0	0	0	0	0	0	0	0	0	0
5	0	6	4	22	8	19	19	1	0	0	0	0	0	0	0	0	0	0	0
6	0	3	8	11	3	20	10	3	0	0	0	0	0	0	0	0	0	0	0
7	0	2	0	10	0	13	1	3	0	0	0	0	0	0	0	0	0	0	0
8	0	4	0	4	0	7	0	1	0	0	0	0	0	0	0	0	0	0	0
9	0	0	0	3	0	5	0	1	0	0	0	0	0	0	0	0	0	0	0
10	0	4	0	2	0	5	0	1	0	0	0	0	0	0	0	0	0	0	0
11	0	0	0	2	0	3	0	1	0	0	0	0	0	0	0	0	0	0	0
12	0	3	0	2	0	4	0	0	0	0	0	0	0	0	0	0	0	0	0
13	0	0	0	1	0	2	0	1	0	0	0	0	0	0	0	0	0	0	0
14	0	3	0	2	0	3	0	0	0	0	0	0	0	0	0	0	0	0	0
15	0	0	0	1	0	2	0	1	0	0	0	0	0	0	0	0	0	0	0
16	0	3	0	2	0	3	0	0	0	0	0	0	0	0	0	0	0	0	0
17	0	0	0	1	0	2	0	1	0	0	0	0	0	0	0	0	0	0	0
18	0	2	0	1	0	2	0	0	0	0	0	0	0	0	0	0	0	0	0

Figure 15. Two-Dimensional Fourier Spectrum (× 100) of f_{ij} After 10, 000 Smoothings of the Form 2 Filter

100 X 2-DIMENSIONAL FOURIER ANALYSIS 10000 SMOOTHINGS FORM 3

WAVE NUMBER E-W

WAVE NUMBER N-S	0	1	2	3	4	5	6	7	8	9	10	11	12	13	14	15	16	17	18
0	0	0	19	0	3	0	21	0	0	0	0	0	0	0	0	0	0	0	0
1	1143	7	61	15	33	15	21	7	0	0	0	0	0	0	0	0	0	0	0
2	0	95	4	69	3	42	9	8	0	0	0	0	0	0	0	0	0	0	0
3	66	2	64	4	52	5	28	5	0	0	0	0	0	0	0	0	0	0	0
4	0	5	19	37	15	39	26	11	0	0	0	0	0	0	0	0	0	0	0
5	77	9	6	33	11	29	22	2	0	0	0	0	0	0	0	0	0	0	0
6	0	6	12	11	7	25	22	2	0	0	0	0	0	0	0	0	0	0	0
7	107	2	5	7	5	3	3	2	0	0	0	0	0	0	0	0	0	0	0
8	0	6	4	4	5	10	13	1	0	0	0	0	0	0	0	0	0	0	0
9	98	2	3	7	3	5	3	1	0	0	0	0	0	0	0	0	0	0	0
10	0	5	2	2	3	7	9	1	0	0	0	0	0	0	0	0	0	0	0
11	78	2	2	6	2	4	3	1	0	0	0	0	0	0	0	0	0	0	0
12	0	5	1	2	2	6	6	1	0	0	0	0	0	0	0	0	0	0	0
13	56	1	2	5	2	4	2	0	0	0	0	0	0	0	0	0	0	0	0
14	0	5	1	2	2	5	4	1	0	0	0	0	0	0	0	0	0	0	0
15	34	1	1	5	1	4	1	0	0	0	0	0	0	0	0	0	0	0	0
16	0	4	0	1	1	5	2	1	0	0	0	0	0	0	0	0	0	0	0
17	11	1	0	5	0	3	0	0	0	0	0	0	0	0	0	0	0	0	0
18	0	3	0	1	0	4	0	0	0	0	0	0	0	0	0	0	0	0	0

Figure 16. Two-Dimensional Fourier Spectrum (× 100) of f_{ij} After 10, 000 Smoothings of the Form 3 Filter

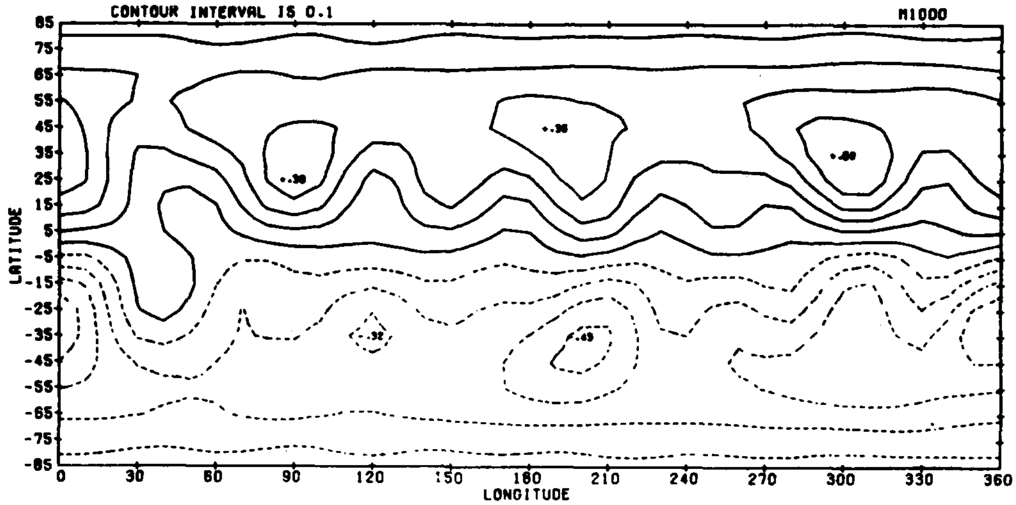

Figure 17. f^*_{ij} After 1000 Applications of the Form 1 Filter

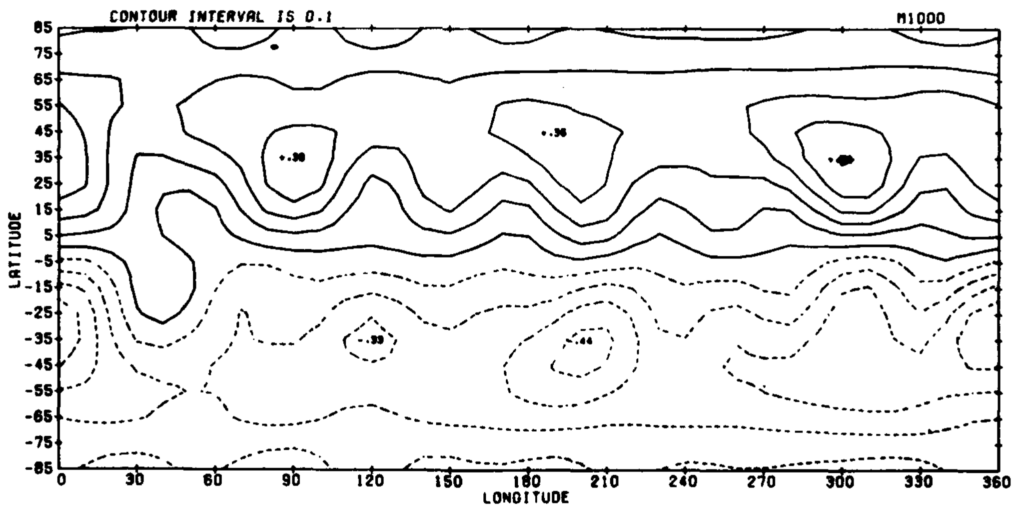

Figure 18. f^*_{ij} After 1000 Applications of the Form 2 Filter

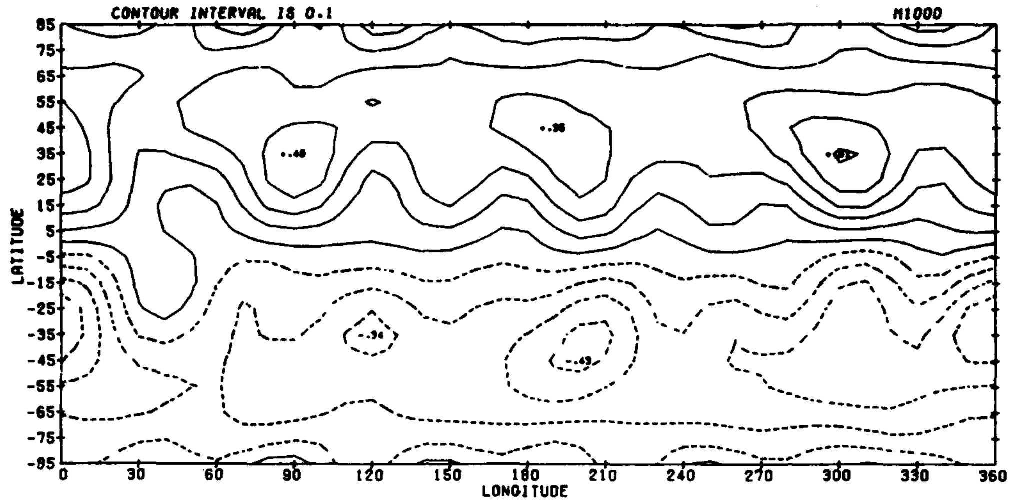

Figure 19. f^*_{ij} After 1000 Applications of the Form 3 Filter

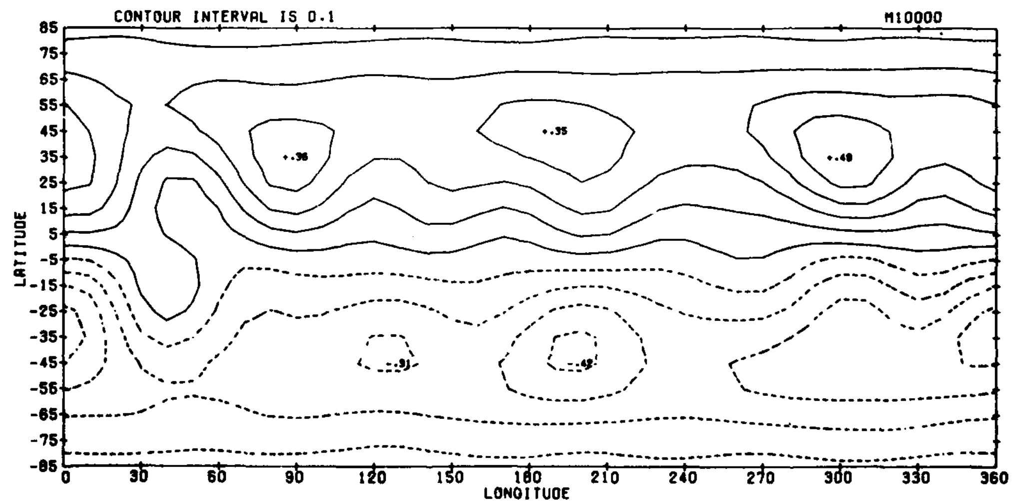

Figure 20. f^*_{ij} After 10,000 Applications of the Form 1 Filter

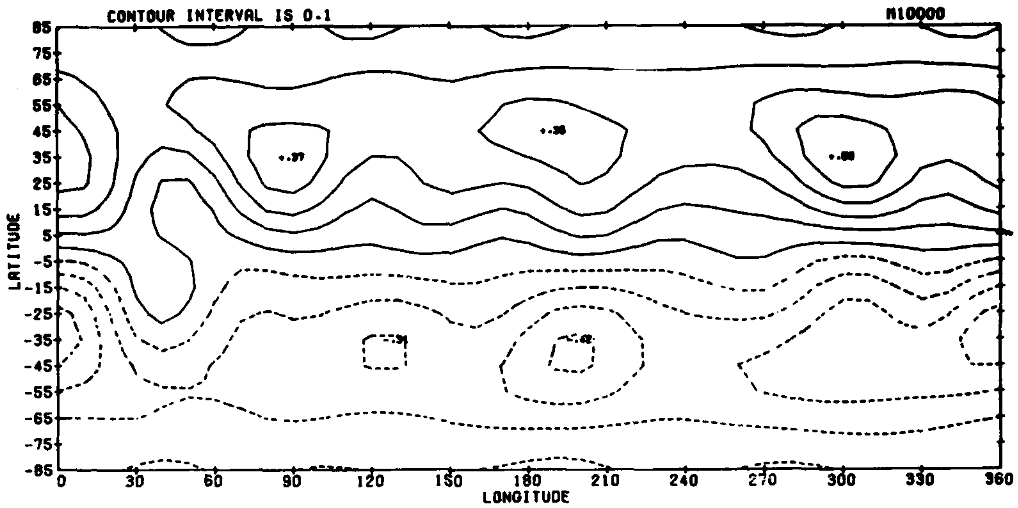

Figure 21. f^*_{ij} After 10, 000 Applications of the Form 2 Filter

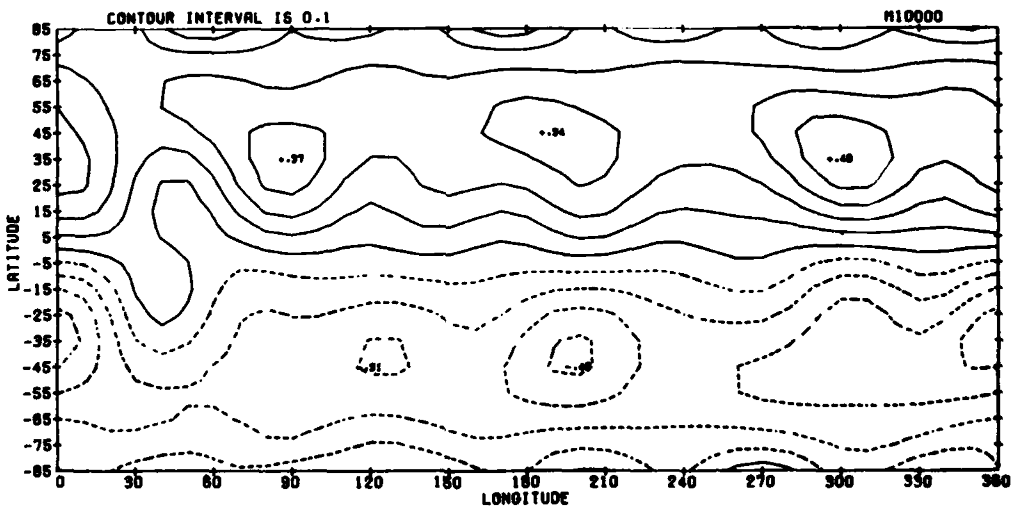

Figure 22. f^*_{ij} After 10, 000 Applications of the Form 3 Filter

100 X RATIO OF FOURIER AMPLITUDES 1000 SMOOTHINGS FORM 1

WAVE NUMBER E-W

WAVE NUMBER N-S	0	1	2	3	4	5	6	7	8	9	10	11	12	13	14	15	16	17	18
0	■	■	100	■	100	■	96	■	43	■	0	■	0	■	0	■	0	■	0
1	100	100	100	100	100	100	98	87	43	2	0	0	0	0	0	0	0	0	0
2	■	100	100	100	100	100	98	87	43	2	0	0	0	0	0	0	0	0	0
3	100	100	100	100	100	100	98	87	43	2	0	0	0	0	0	0	0	0	0
4	■	100	100	100	100	100	98	87	43	2	0	0	0	0	0	0	0	0	0
5	100	100	100	100	100	100	98	87	43	2	0	0	0	0	0	0	0	0	0
6	■	98	98	98	98	98	97	86	42	2	0	0	0	0	0	0	0	0	0
7	87	87	87	87	87	87	86	76	37	2	0	0	0	0	0	0	0	0	0
8	■	43	43	43	43	43	42	37	18	1	0	0	0	0	0	0	0	0	0
9	2	2	2	2	2	2	2	2	1	0	0	0	0	0	0	0	0	0	0
10	■	0	0	0	0	0	0	0	0	0	0	0	0	0	0	0	0	0	0
11	0	0	0	0	0	0	0	0	0	0	0	0	0	0	0	0	0	0	0
12	■	0	0	0	0	0	0	0	0	0	0	0	0	0	0	0	0	0	0
13	0	0	0	0	0	0	0	0	0	0	0	0	0	0	0	0	0	0	0
14	■	0	0	0	0	0	0	0	0	0	0	0	0	0	0	0	0	0	0
15	0	0	0	0	0	0	0	0	0	0	0	0	0	0	0	0	0	0	0
16	■	0	0	0	0	0	0	0	0	0	0	0	0	0	0	0	0	0	0
17	0	0	0	0	0	0	0	0	0	0	0	0	0	0	0	0	0	0	0
18	■	0	■	0	■	0	■	0	■	0	■	0	■	0	■	0	■	0	■

Figure 23. Percent of Initial Fourier Amplitudes, f^*_{ij}, Remaining After 1000 Applications of Form 1 Filter

100 X RATIO OF FOURIER AMPLITUDES 1000 SMOOTHINGS FORM 2

WAVE NUMBER E-W

WAVE NUMBER N-S	0	1	2	3	4	5	6	7	8	9	10	11	12	13	14	15	16	17	18
0	■	■	103	■	107	■	112	■	50	■	0	■	0	■	0	■	0	■	0
1	102	100	99	100	101	100	91	87	41	2	0	0	0	0	0	0	0	0	0
2	■	100	65	100	76	100	81	87	34	2	0	0	0	0	0	0	0	0	0
3	97	100	101	100	99	100	103	87	44	2	0	0	0	0	0	0	0	0	0
4	■	100	95	100	124	100	133	87	31	2	0	0	0	0	0	0	0	0	0
5	83	100	97	100	108	100	90	87	40	2	0	0	0	0	0	0	0	0	0
6	■	100	106	99	193	99	174	86	52	2	0	0	0	0	0	0	0	0	0
7	48	92	223	93	121	94	99	83	42	2	0	0	0	0	0	0	0	0	0
8	■	68	5	62	21	55	21	69	7	1	0	0	0	0	0	0	0	0	0
9	0	36	0	136	0	78	0	11	0	0	0	0	0	0	0	0	0	0	0
10	■	25	0	155	0	60	0	25	0	1	0	0	0	0	0	0	0	0	0
11	0	23	0	22	0	29	0	19	0	0	0	0	0	0	0	0	0	0	0
12	■	18	0	14	0	11	0	21	0	2	0	0	0	0	0	0	0	0	0
13	0	164	0	23	0	22	0	24	0	0	0	0	0	0	0	0	0	0	0
14	■	11	0	8	0	6	0	17	0	1	0	0	0	0	0	0	0	0	0
15	0	24	0	113	0	33	0	17	0	0	0	0	0	0	0	0	0	0	0
16	■	56	0	48	0	6	0	22	0	1	0	0	0	0	0	0	0	0	0
17	0	26	0	139	0	36	0	28	0	0	0	0	0	0	0	0	0	0	0
18	■	7	■	9	■	7	■	29	■	1	■	0	■	0	■	0	■	0	■

Figure 24. Percent of Initial Fourier Amplitudes, f^*_{ij}, Remaining After 1000 Applications of Form 2 Filter

100 X RATIO OF FOURIER AMPLITUDES 1000 SMOOTHINGS FORM 3

WAVE NUMBER E-W

WAVE NUMBER N-S	0	1	2	3	4	5	6	7	8	9	10	11	12	13	14	15	16	17	18
0	■	■	114	■	113	■	109	■	57	■	0	■	0	■	0	■	0	■	0
1	100	98	99	102	111	106	81	92	41	2	0	0	0	0	0	0	0	0	0
2	■	100	39	100	87	102	86	89	36	2	0	0	0	0	0	0	0	0	0
3	100	82	101	107	94	134	115	64	55	1	0	0	0	0	0	0	0	0	0
4	■	99	80	99	109	95	119	83	17	2	0	0	0	0	0	0	0	0	0
5	100	112	97	95	137	75	64	217	29	2	0	0	0	0	0	0	0	0	0
6	■	122	129	114	149	121	158	103	62	3	0	0	0	0	0	0	0	0	0
7	100	47	448	102	226	127	153	149	66	3	0	0	0	0	0	0	0	0	0
8	■	60	192	116	52	32	41	93	19	1	0	0	0	0	0	0	0	0	0
9	100	8	83	177	41	166	67	56	31	1	0	0	0	0	0	0	0	0	0
10	■	38	70	315	32	103	20	35	20	1	0	0	0	0	0	0	0	0	0
11	100	6	20	28	18	57	45	68	29	0	0	0	0	0	0	0	0	0	0
12	■	37	41	27	18	24	11	30	7	1	0	0	0	0	0	0	0	0	0
13	100	57	29	31	32	43	60	80	18	0	0	0	0	0	0	0	0	0	0
14	■	26	202	16	12	16	3	25	6	0	0	0	0	0	0	0	0	0	0
15	100	9	6	148	7	65	29	55	6	0	0	0	0	0	0	0	0	0	0
16	■	160	21	98	2	17	2	32	10	0	0	0	0	0	0	0	0	0	0
17	100	10	2	183	1	71	4	92	2	1	0	0	0	0	0	0	0	0	0
18	■	19	■	19	■	18	■	44	■	1	■	0	■	0	■	0	■	0	■

Figure 25. Percent of Initial Fourier Amplitudes, f^*_{ij}, Remaining After 1000 Applications of Form 3 Filter

100 X RATIO OF FOURIER AMPLITUDES 10000 SMOOTHINGS FORM 1

WAVE NUMBER E-W

WAVE NUMBER N-S	0	1	2	3	4	5	6	7	8	9	10	11	12	13	14	15	16	17	18
0	■	■	100	■	100	■	86	■	0	■	0	■	0	■	0	■	0	■	0
1	100	100	100	100	100	99	86	25	0	0	0	0	0	0	0	0	0	0	0
2	■	100	100	100	100	99	86	25	0	0	0	0	0	0	0	0	0	0	0
3	100	100	100	100	100	99	86	25	0	0	0	0	0	0	0	0	0	0	0
4	■	100	100	100	100	99	86	25	0	0	0	0	0	0	0	0	0	0	0
5	99	99	99	99	99	98	85	25	0	0	0	0	0	0	0	0	0	0	0
6	■	86	86	86	86	85	74	22	0	0	0	0	0	0	0	0	0	0	0
7	25	25	25	25	25	25	22	6	0	0	0	0	0	0	0	0	0	0	0
8	■	0	0	0	0	0	0	0	0	0	0	0	0	0	0	0	0	0	0
9	0	0	0	0	0	0	0	0	0	0	0	0	0	0	0	0	0	0	0
10	■	0	0	0	0	0	0	0	0	0	0	0	0	0	0	0	0	0	0
11	0	0	0	0	0	0	0	0	0	0	0	0	0	0	0	0	0	0	0
12	■	0	0	0	0	0	0	0	0	0	0	0	0	0	0	0	0	0	0
13	0	0	0	0	0	0	0	0	0	0	0	0	0	0	0	0	0	0	0
14	■	0	0	0	0	0	0	0	0	0	0	0	0	0	0	0	0	0	0
15	0	0	0	0	0	0	0	0	0	0	0	0	0	0	0	0	0	0	0
16	■	0	0	0	0	0	0	0	0	0	0	0	0	0	0	0	0	0	0
17	0	0	0	0	0	0	0	0	0	0	0	0	0	0	0	0	0	0	0
18	■	0	■	0	■	0	■	0	■	0	■	0	■	0	■	0	■	0	■

Figure 26. Percent of Initial Fourier Amplitudes, f^*_{ij}, Remaining After 10,000 Smoothings of Form 1 Filter

100 X RATIO OF FOURIER AMPLITUDES 10000 SMOOTHINGS FORM 2

WAVE NUMBER E-W

WAVE NUMBER N-S	0	1	2	3	4	5	6	7	8	9	10	11	12	13	14	15	16	17	18
0	■	■	95	■	103	■	95	■	0	■	0	■	0	■	0	■	0	■	0
1	103	100	99	100	94	99	96	25	0	0	0	0	0	0	0	0	0	0	0
2	■	100	125	100	77	99	74	25	0	0	0	0	0	0	0	0	0	0	0
3	94	100	101	100	104	99	80	25	0	0	0	0	0	0	0	0	0	0	0
4	■	100	110	100	125	99	111	25	0	0	0	0	0	0	0	0	0	0	0
5	70	100	95	100	83	99	106	25	0	0	0	0	0	0	0	0	0	0	0
6	■	97	70	93	169	93	118	23	0	0	0	0	0	0	0	0	0	0	0
7	2	32	10	46	6	50	4	16	0	0	0	0	0	0	0	0	0	0	0
8	■	63	0	123	0	58	0	8	0	0	0	0	0	0	0	0	0	0	0
9	0	3	0	53	0	50	0	6	0	0	0	0	0	0	0	0	0	0	0
10	■	35	0	288	0	142	0	3	0	0	0	0	0	0	0	0	0	0	0
11	0	5	0	7	0	16	0	6	0	0	0	0	0	0	0	0	0	0	0
12	■	32	0	24	0	31	0	3	0	0	0	0	0	0	0	0	0	0	0
13	0	50	0	7	0	11	0	7	0	0	0	0	0	0	0	0	0	0	0
14	■	22	0	14	0	20	0	2	0	0	0	0	0	0	0	0	0	0	0
15	0	8	0	32	0	16	0	5	0	0	0	0	0	0	0	0	0	0	0
16	■	133	0	84	0	21	0	3	0	0	0	0	0	0	0	0	0	0	0
17	0	9	0	39	0	18	0	8	0	0	0	0	0	0	0	0	0	0	0
18	■	16	■	16	■	21	■	4	■	0	■	0	■	0	■	0	■	0	■

Figure 27. Percent of Initial Fourier Amplitudes, f^*_{ij}, Remaining After 10,000 Smoothings of Form 2 Filter

100 X RATIO OF FOURIER AMPLITUDES 10000 SMOOTHINGS FORM 3

WAVE NUMBER E-W

WAVE NUMBER N-S	0	1	2	3	4	5	6	7	8	9	10	11	12	13	14	15	16	17	18
0	■	■	109	■	163	■	122	■	0	■	0	■	0	■	0	■	0	■	0
1	100	93	101	90	101	89	112	25	0	0	0	0	0	0	0	0	0	0	0
2	■	100	61	100	53	100	44	24	0	0	0	0	0	0	0	0	0	0	0
3	100	43	99	92	100	143	73	27	0	0	0	0	0	0	0	0	0	0	0
4	■	98	88	100	162	97	169	27	0	0	0	0	0	0	0	0	0	0	0
5	100	140	106	148	109	151	126	36	0	0	0	0	0	0	0	0	0	0	0
6	■	115	108	96	464	116	258	16	0	0	0	0	0	0	0	0	0	0	0
7	100	90	469	36	117	14	26	9	0	0	0	0	0	0	0	0	0	0	0
8	■	87	229	142	49	90	51	6	0	0	0	0	0	0	0	0	0	0	0
9	100	66	77	151	24	58	26	3	0	0	0	0	0	0	0	0	0	0	0
10	■	53	70	338	59	224	57	3	0	0	0	0	0	0	0	0	0	0	0
11	100	60	18	30	10	24	20	3	0	0	0	0	0	0	0	0	0	0	0
12	■	52	39	29	41	49	42	3	0	0	0	0	0	0	0	0	0	0	0
13	100	485	24	35	18	20	28	4	0	0	0	0	0	0	0	0	0	0	0
14	■	37	190	16	32	32	13	2	0	0	0	0	0	0	0	0	0	0	0
15	100	76	5	176	4	31	14	2	0	0	0	0	0	0	0	0	0	0	0
16	■	226	19	100	6	33	8	3	0	0	0	0	0	0	0	0	0	0	0
17	100	83	1	220	1	34	2	4	0	0	0	0	0	0	0	0	0	0	0
18	■	27	■	19	■	35	■	4	■	0	■	0	■	0	■	0	■	0	■

Figure 28. Percent of Initial Fourier Amplitudes, f^*_{ij}, Remaining After 10,000 Smoothings of Form 3 Filter

100 X RATIO OF FOURIER AMPLITUDES 1000 SMOOTHINGS FORM 4

WAVE NUMBER E-W

WAVE NUMBER N-S \ E-W	0	1	2	3	4	5	6	7	8	9	10	11	12	13	14	15	16	17	18
0	■	■	103	■	107	■	113	■	50	■	0	■	0	■	0	■	0	■	0
1	102	100	99	100	101	100	91	87	41	2	0	0	0	0	0	0	0	0	0
2	■	100	85	100	76	100	80	87	34	2	0	0	0	0	0	0	0	0	0
3	97	100	101	100	99	100	103	87	44	2	0	0	0	0	0	0	0	0	0
4	■	100	95	100	124	100	134	87	31	2	0	0	0	0	0	0	0	0	0
5	83	100	97	100	108	100	90	87	40	2	0	0	0	0	0	0	0	0	0
6	■	100	106	99	196	99	175	86	52	2	0	0	0	0	0	0	0	0	0
7	47	91	221	93	119	94	98	83	42	2	0	0	0	0	0	0	0	0	0
8	■	67	5	62	20	53	20	69	7	1	0	0	0	0	0	0	0	0	0
9	0	35	0	136	0	79	0	12	0	0	0	0	0	0	0	0	0	0	0
10	■	25	0	155	0	58	0	24	0	1	0	0	0	0	0	0	0	0	0
11	0	22	0	22	0	29	0	20	0	0	0	0	0	0	0	0	0	0	0
12	■	18	0	14	0	10	0	20	0	2	0	0	0	0	0	0	0	0	0
13	0	160	0	23	0	22	0	25	0	0	0	0	0	0	0	0	0	0	0
14	■	10	0	8	0	6	0	17	0	1	0	0	0	0	0	0	0	0	0
15	0	24	0	113	0	33	0	17	0	0	0	0	0	0	0	0	0	0	0
16	■	55	0	48	0	6	0	21	0	1	0	0	0	0	0	0	0	0	0
17	0	25	0	138	0	36	0	29	0	0	0	0	0	0	0	0	0	0	0
18	■	6	■	9	■	6	■	29	■	1	■	0	■	0	■	0	■	0	■

Figure 29. Percent of Initial Fourier Amplitudes, f^*_{ij}, Remaining After 1000 Applications of Form 4 Filter

100 X RATIO OF FOURIER AMPLITUDES 1000 SMOOTHINGS FORM 5

WAVE NUMBER E-W

WAVE NUMBER N-S \ E-W	0	1	2	3	4	5	6	7	8	9	10	11	12	13	14	15	16	17	18
0	■	■	100	■	100	■	99	■	43	■	0	■	0	■	0	■	0	■	0
1	100	100	100	100	100	100	98	87	43	2	0	0	0	0	0	0	0	0	0
2	■	100	99	100	99	100	98	87	42	2	0	0	0	0	0	0	0	0	0
3	100	99	100	99	100	100	99	87	43	2	0	0	0	0	0	0	0	0	0
4	■	100	100	100	101	100	100	87	42	2	0	0	0	0	0	0	0	0	0
5	99	102	100	101	101	100	98	90	43	2	0	0	0	0	0	0	0	0	0
6	■	100	100	100	96	101	110	84	44	2	0	0	0	0	0	0	0	0	0
7	86	77	117	86	100	90	93	86	40	2	0	0	0	0	0	0	0	0	0
8	■	38	10	37	45	36	43	46	15	1	0	0	0	0	0	0	0	0	0
9	25	7	4	33	3	22	7	5	3	0	0	0	0	0	0	0	0	0	0
10	■	4	2	18	7	9	6	3	1	0	0	0	0	0	0	0	0	0	0
11	14	1	1	1	1	2	2	2	1	0	0	0	0	0	0	0	0	0	0
12	■	1	1	1	2	0	1	1	0	0	0	0	0	0	0	0	0	0	0
13	11	3	1	1	1	1	1	1	0	0	0	0	0	0	0	0	0	0	0
14	■	1	3	0	1	0	0	0	0	0	0	0	0	0	0	0	0	0	0
15	9	0	0	2	0	1	0	1	0	0	0	0	0	0	0	0	0	0	0
16	■	3	0	1	0	0	0	0	0	0	0	0	0	0	0	0	0	0	0
17	9	0	0	2	0	1	0	1	0	0	0	0	0	0	0	0	0	0	0
18	■	0	■	0	■	0	■	0	■	0	■	0	■	0	■	0	■	0	■

Figure 30. Percent of Initial Fourier Amplitudes, f^*_{ij}, Remaining After 1000 Applications of Form 5 Filter

100 X RATIO OF FOURIER AMPLITUDES 10000 SMOOTHINGS FORM 4

WAVE NUMBER E-W

WAVE NUMBER N-S	0	1	2	3	4	5	6	7	8	9	10	11	12	13	14	15	16	17	18
0	■	■	94	■	103	■	95	■	0	■	0	■	0	■	0	■	0	■	0
1	103	100	99	100	94	99	96	25	0	0	0	0	0	0	0	0	0	0	0
2	■	100	126	100	78	99	74	25	0	0	0	0	0	0	0	0	0	0	0
3	94	100	101	100	104	99	80	25	0	0	0	0	0	0	0	0	0	0	0
4	■	100	110	100	125	99	111	25	0	0	0	0	0	0	0	0	0	0	0
5	70	100	95	100	83	99	106	25	0	0	0	0	0	0	0	0	0	0	0
6	■	96	69	93	167	93	116	23	0	0	0	0	0	0	0	0	0	0	0
7	2	30	9	44	5	49	4	15	0	0	0	0	0	0	0	0	0	0	0
8	■	63	0	122	0	58	0	8	0	0	0	0	0	0	0	0	0	0	0
9	0	4	0	50	0	48	0	5	0	0	0	0	0	0	0	0	0	0	0
10	■	35	0	287	0	142	0	3	0	0	0	0	0	0	0	0	0	0	0
11	0	6	0	7	0	15	0	6	0	0	0	0	0	0	0	0	0	0	0
12	■	32	0	24	0	31	0	3	0	0	0	0	0	0	0	0	0	0	0
13	0	55	0	6	0	10	0	7	0	0	0	0	0	0	0	0	0	0	0
14	■	22	0	14	0	20	0	2	0	0	0	0	0	0	0	0	0	0	0
15	0	9	0	30	0	15	0	5	0	0	0	0	0	0	0	0	0	0	0
16	■	133	0	83	0	21	0	3	0	0	0	0	0	0	0	0	0	0	0
17	0	10	0	36	0	17	0	8	0	0	0	0	0	0	0	0	0	0	0
18	■	18	■	16	■	21	■	4	■	0	■	0	■	0	■	0	■	0	■

Figure 31. Percent of Initial Fourier Amplitudes, f^*_{ij}, remaining After 10, 000 Smoothings of Form 4 Filter

100 X RATIO OF FOURIER AMPLITUDES 10000 SMOOTHINGS FORM 5

WAVE NUMBER E-W

WAVE NUMBER N-S	0	1	2	3	4	5	6	7	8	9	10	11	12	13	14	15	16	17	18
0	■	■	100	■	100	■	86	■	0	■	0	■	0	■	0	■	0	■	0
1	100	100	100	99	100	98	86	25	0	0	0	0	0	0	0	0	0	0	0
2	■	100	101	100	98	99	85	25	0	0	0	0	0	0	0	0	0	0	0
3	100	97	100	94	100	97	85	26	0	0	0	0	0	0	0	0	0	0	0
4	■	100	101	100	103	99	89	26	0	0	0	0	0	0	0	0	0	0	0
5	96	104	99	107	97	108	90	28	0	0	0	0	0	0	0	0	0	0	0
6	■	89	87	86	94	88	95	20	0	0	0	0	0	0	0	0	0	0	0
7	42	9	100	17	40	20	18	7	0	0	0	0	0	0	0	0	0	0	0
8	■	15	40	27	2	14	3	2	0	0	0	0	0	0	0	0	0	0	0
9	16	1	3	2	2	3	1	0	0	0	0	0	0	0	0	0	0	0	0
10	■	3	4	18	1	9	1	0	0	0	0	0	0	0	0	0	0	0	0
11	10	1	0	0	0	0	0	0	0	0	0	0	0	0	0	0	0	0	0
12	■	1	1	1	0	1	1	0	0	0	0	0	0	0	0	0	0	0	0
13	8	4	0	0	0	0	0	0	0	0	0	0	0	0	0	0	0	0	0
14	■	1	4	0	0	0	0	0	0	0	0	0	0	0	0	0	0	0	0
15	7	0	0	1	0	0	0	0	0	0	0	0	0	0	0	0	0	0	0
16	■	3	0	1	0	0	0	0	0	0	0	0	0	0	0	0	0	0	0
17	7	0	0	1	0	0	0	0	0	0	0	0	0	0	0	0	0	0	0
18	■	0	■	0	■	0	■	0	■	0	■	0	■	0	■	0	■	0	■

Figure 32. Percent of Initial Fourier Amplitudes, f^*_{ij}, Remaining After 10, 000 Smoothings of Form 5 Filter

5. CONCLUSIONS

Among the five forms of the filter which were tested on noisy fields on the surface of a sphere, Form 1, the simplest form, stands out as superior. Form 3, which has a tendency to pathological behavior near the poles is inferior and should be avoided. Forms 2, 4 and 5 appear to be quite similar in their effects.

In applications, the order of the filter, p, should be chosen so that there is a sharp transition between those Fourier components which are considered undesirable (and are strongly damped) and those components which one wishes to remain unaffected by the filtering process.

References

1. Shapiro, R. (1971) The use of linear filtering as a parameterization of atmospheric diffusion, J. Atmos. Sci. 28:523-531.
2. Shapiro, R. (1975) Linear filtering, Math. Comp. 29:1094-1097.
3. Hunt, B.G. (1974) A global general circulation model of the atmosphere based on the semi-spectral method, Mon. Wea. Rev. 102:3-16.
4. Francis, P.E. (1975) The use of a multipoint filter as a dissipative mechanism in a numerical model of the general circulation of the atmosphere, Quart. J. R. Met. Soc. 101:567-582.
5. Voice, M.E., and Hunt, B.G. (1975) Southern hemisphere forecasting experiments with a semi-spectral model, Mon. Wea. Rev. 103:1077-1088.
6. Tapp, M.C., and White, P.W. (1976) A non-hydrostatic mesoscale model, Quart. J. R. Met. Soc. 102:277-296.
7. Mudrick, S. (1976) On the use of a scale-dependent filter in channel model integrations, J. Comp. Phys. 20:33-49.
8. Mudrick, S. (1978) A further test of a scale-dependent filter for use in finite-difference modeling, Mon. Wea. Rev. 106:1205-1211.
9. Kalnay-Rivas, E., Bayliss, A., and Storch, J. (1977) The 4th order GISS model of the global atmosphere, Contrib. to Atmos. Phys. 50:299-311.
10. Yee, S.Y.K. (1978) An Efficient Barotropic Vorticity Equation Model on a Sphere, Env. Res. Pap. No. 645, AFGL-TR-78-0273, AD A065 117.